

Improvements in Geomembrane Protection Efficiency Using Cushioning Geotextiles

R. A. Austin

Geosynthetic Centre of Excellence, Geofabrics Australasia Pty Ltd, Gold Coast, Australia

D. T. Gibbs, and P. M. Kendall

Keywords: Geomembrane, Protection Efficiency, Scan, Strain, Cushioning

ABSTRACT: The use of geotextiles as protection layers for geomembranes in lining applications is a common use for geotextiles and minimising installation damage, in-service damage and geomembrane strain is critical for the long-term performance of the lining system. In such applications, protection of the membrane from localised point loads caused by the overlying drainage stone thus minimising potential for environmental stress cracking is desirable, if the long-term performance of the liner is to be assured.

The paper reports on the extensive testing of different types of geotextiles for liner protection applications. The testing reported followed the ASTM D5514-06 test procedure modified to include the use of a fixed stone profile and uniform pneumatic load application.

To ensure a consistent stone arrangement and loading onto the liner, fixed stone profiles were created using fibre-reinforced resin to hold the drainage stone in a rigid arrangement, yet provide a natural stone surface texture similar to that of stone as placed on site. Using this approach, different liner and geotextile combinations could be tested against the same stone profile and loading conditions, thus enabling easy comparison of damage and recorded strain.

Test results are presented and compared for both staple fibre and continuous filament geotextiles and the effect of different polymer types is discussed.

1 INTRODUCTION

The use of geotextiles as cushioning and protection layers for geomembranes has been a significant application for geotextiles since the early use of geomembrane liners in landfills and hazardous waste containment facilities. Protection of the liner from physical damage and strain induced by adjacent drainage stone is vital if the long-term durability of the liner is to be assured and environmental stress cracking avoided.

This paper summarises testing carried out using different types of geotextiles as cushioning layers between drainage stone and a geomembrane using a modified version of the ASTM D5514-06 (2011) procedure with strain measurements undertaken by the use of a laser scanning on a metal indicator sheet.

This paper furthers initial studies reported by Hornsey and Gallagher (2012), Hornsey and Wishaw (2012) and Hornsey (2013) including additional test results on the same rock profile. The total data set generated includes results for material from different textile types and producers.

1.1 Test Methodology

The analysis was carried out in accordance with the ASTM D5514-06 (2011) procedure, modified to include the use of a fixed stone profile and laser scanning for the determination of geomembrane strain, Figure 1. The 450mm diameter fixed stone profile was selected to ensure the stone arrangement and loading applied to the liner sample in different tests was the same, allowing direct comparison of results. The laser scanning approach was used for strain measurement as it provided a quick and repeatable method of strain analysis across the whole contoured surface of the membrane rather than relying on visual pre-selection of the highest strain regions of the membrane for detailed manual analysis. The test procedure uses air pressure to load the geomembrane to the correct test load and push it onto the protection layer and drainage stone. Following loading the air pressure is released, the test samples removed and the strain indicator sheet sent for laser scanning and the strain in the liner calculated.

As per Figure 2, the geosynthetic material profile under test is inverted in the test rig with the stone profile installed in the base of the rig underlying the protection geotextile and membrane sample. Inverting the materials in this way, from their orientation onsite, permits easy installation in the test rig and enables the lower and upper halves of the test rig to seal against the geomembrane during closure of the rig with minimal effects on the membrane. To eliminate the influence of restraining the membrane, strain measurements are only recorded for the central 350mm diameter of the test specimen. This configuration does not account for any support which may be provided by a subgrade material and therefore is a conservative approach. The development of this test procedure, the repeatability of results for the fixed stone arrangement and the accuracy of the laser scanning technique have been documented by Hornsey & Wishaw (2012).

Extending earlier work reported by Hornsey (2013) on the testing of 40 different geotextiles from various manufacturers and of different types used as cushioning layers, additional products were assessed and their performance evaluated under the following conditions:

- 1) 20-75mm igneous aggregate (fixed)
- 2) 2mm smooth HDPE geomembrane
- 3) 0.3mm aluminium recording plate
- 4) 600kPa confining pressure
- 5) 24 hour loading period.



Figure 1. Fixed stone profile

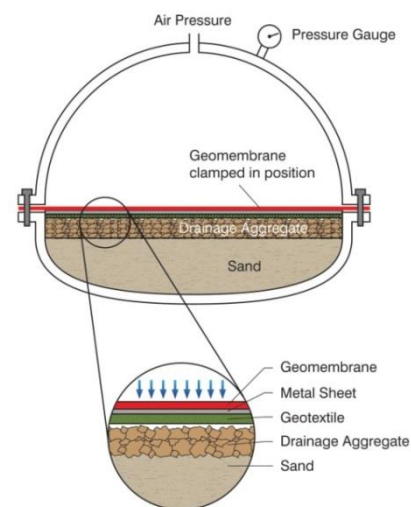


Figure 2. Test configuration

2 RESULTS

Historically, mass and thickness have been used as general indicators of a geotextiles ability to protect geomembranes from local and global strain. The early combined dataset provided by Hornsey (2013) showed a low R^2 value classified and as unacceptable with a Cronbach's $\alpha < 5.0$. While this correlation has improved with the additional test data, it is still classified as poor (Figure 3).

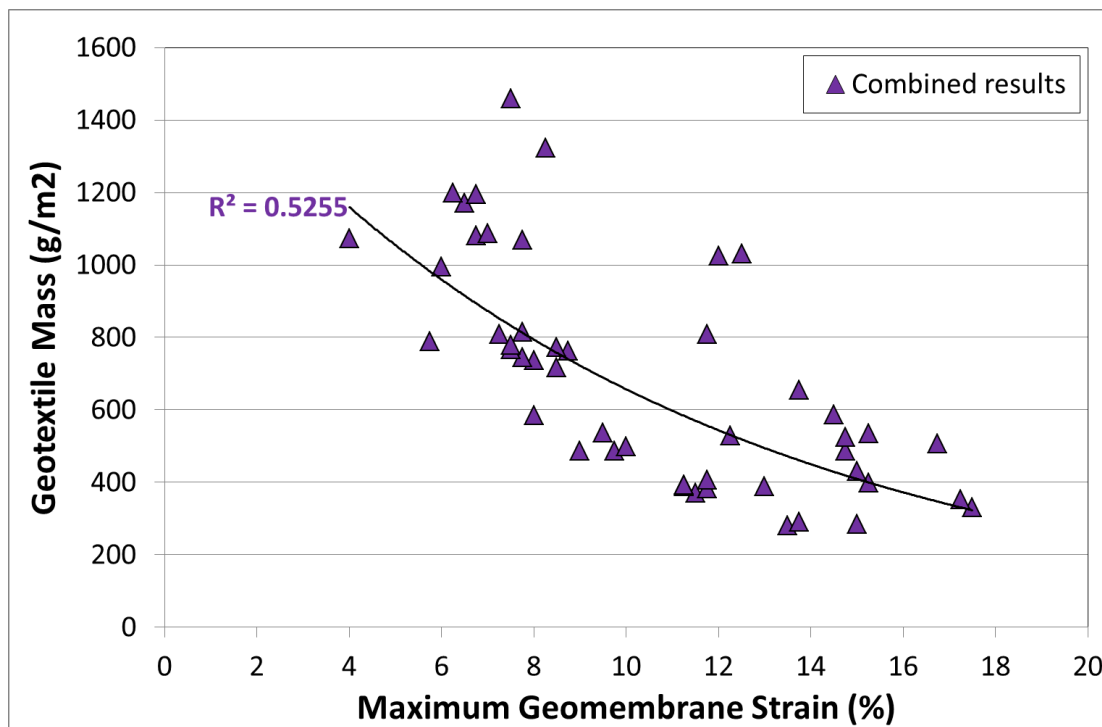


Figure 3. Mass vs strain relationship for complete data set

When the data are split into geotextiles of different manufacturing method and polymer type, however, the correlations improve. This analysis is detailed below.

2.1 Influence of Manufacturing Method

There are two main methods of manufacturing nonwoven geotextiles. The first method uses short-cut staple fibres which come in a variety of polymer types with different tenacities, elongations, thicknesses, staple lengths, crimp levels etc. The second method utilizes fibres extruded from base polymer chip to form long continuous lengths. Both methods use needle-punching technology to lock the fibres together to form a dense geotextile after which the fibres may or may not be heat set.

Analysis was undertaken to understand the performance of both staple fibre (SF) and continuous filament (CF) geotextiles of two primary polymer types when subjected to the same loading conditions. Geotextiles were selected from a variety of different countries and manufacturers and include a mass range of 281 – 1,459 g/m^2 . Mass and thickness measurements were taken in accordance with AS 3706.1. For clarity, the data was split into 3 families of products based on polymer type and production method:

- 1) SF PP : Staple Fibre Polypropylene
- 2) CF PP : Continuous Filament Polypropylene
- 3) CF PET : Continuous Filament Polyester

Early review of the scan data revealed the limitation of the scanning equipment to be around 0.05% of the area. Values beyond this level appeared anomalous and, as such, were ignored in the assessment of maximum strain. Numerical values of the maximum strains recorded are presented in Table 1.

Table 1. Geotextile mass, thickness and recorded maximum geomembrane strain data

Test No.	Staple Fibre Polypropylene (SF PP)			Test No.	Continuous Filament Polypropylene (CF PP)			Test No.	Continuous Filament Polypropylene (CF PET)		
	Mass	Thick	Max. Strain		Mass	Thick	Max. Strain		Mass	Thick	Max. Strain
	<i>g/m²</i>	<i>mm</i>	<i>%</i>		<i>g/m²</i>	<i>mm</i>	<i>%</i>		<i>g/m²</i>	<i>mm</i>	<i>%</i>
1	331	1.87	17.50	15	399	3.09	15.25	28	<i>281</i>	<i>1.62</i>	<i>13.50</i>
2	352	1.65	17.25	16	528	4.20	12.25	29	<i>284</i>	<i>1.62</i>	<i>15.00</i>
3	430	4.66	15.00	17	717	4.27	8.50	30	<i>291</i>	<i>1.98</i>	<i>13.75</i>
4	486	4.93	14.75	18	763	5.66	8.75	31	<i>370</i>	<i>2.67</i>	<i>11.50</i>
5	506	3.99	16.75	19	773	5.78	8.50	32	<i>383</i>	<i>2.77</i>	<i>11.75</i>
6	524	4.80	14.75	20	808	6.22	7.25	33	<i>388</i>	<i>2.55</i>	<i>13.00</i>
7	535	3.72	15.25	21	815	5.57	7.75	34	<i>389</i>	<i>2.70</i>	<i>11.25</i>
8	586	5.09	14.50	22	1070	7.06	7.75	35	<i>392</i>	<i>2.83</i>	<i>11.25</i>
9	655	4.92	13.75	23	1081	7.77	6.75	36	<i>393</i>	<i>3.50</i>	<i>11.25</i>
10	808	6.59	11.75	24	1087	7.11	7.00	37	<i>406</i>	<i>2.74</i>	<i>11.75</i>
11	1026	8.12	12.00	25	1172	7.33	6.50	38	<i>486</i>	<i>3.93</i>	<i>9.00</i>
12	1032	7.46	12.50	26	1196	7.57	6.75	39	<i>486</i>	<i>3.80</i>	<i>9.75</i>
13	1324	8.68	8.25	27	1199	7.56	6.25	40	<i>499</i>	<i>4.65</i>	<i>10.00</i>
14	1459	8.62	7.50					41	<i>537</i>	<i>3.74</i>	<i>9.50</i>
								42	<i>585</i>	<i>4.27</i>	<i>8.00</i>
								43	<i>737</i>	<i>5.49</i>	<i>8.00</i>
								44	<i>744</i>	<i>5.78</i>	<i>7.75</i>
								45	<i>767</i>	<i>5.62</i>	<i>7.50</i>
								46	<i>778</i>	<i>5.52</i>	<i>7.50</i>
								47	<i>788</i>	<i>5.86</i>	<i>5.75</i>
								48	<i>996</i>	<i>5.03</i>	<i>6.00</i>
								49	<i>1074</i>	<i>6.99</i>	<i>4.00</i>

Note: *Italicised values for Test Numbers 28, 29,30 ,38, 39,40, 44,45 and 49 represent new data*
 Other values as reported by Hornsey (2013)

Plotting the Table 1 data graphically permits a visual understanding of the mass/strain and thickness/strain relationships such that clear differences between the performances of the product groups can be identified (Figures 4 & 5). Best fit trendlines were used to enhance the relationships between each product type. Additionally, maximum strain values for each test were generated from the 3D scan data and the results processed to allow cumulative presentation of strain results.

Frequently landfill and other liner project specifications for geotextile cushioning layers specify material requirements based on geotextile mass alone or mass and other mechanical properties without any reference to proven test performance. From the testing reported, it is clear that mass alone is not a suitable parameter on which to base a material procurement specification, rather the results show that a material performance specification based on testing with project specific material should be used. Referring to Figure 4, the results for the 3 No. product groupings presented show distinctly different level of performance in terms of their ability to limit maximum strain in the liner. Using the curves for each dataset, by interpolation an 800 g/m² geotextile would result in maximum strains of 6.5%, 8.9% or 12.2% for the CF PET, CF PP and SF PP product groups respectively. Similar large differences in recorded strain were achieved between different product families of similar mass, Figure 5.

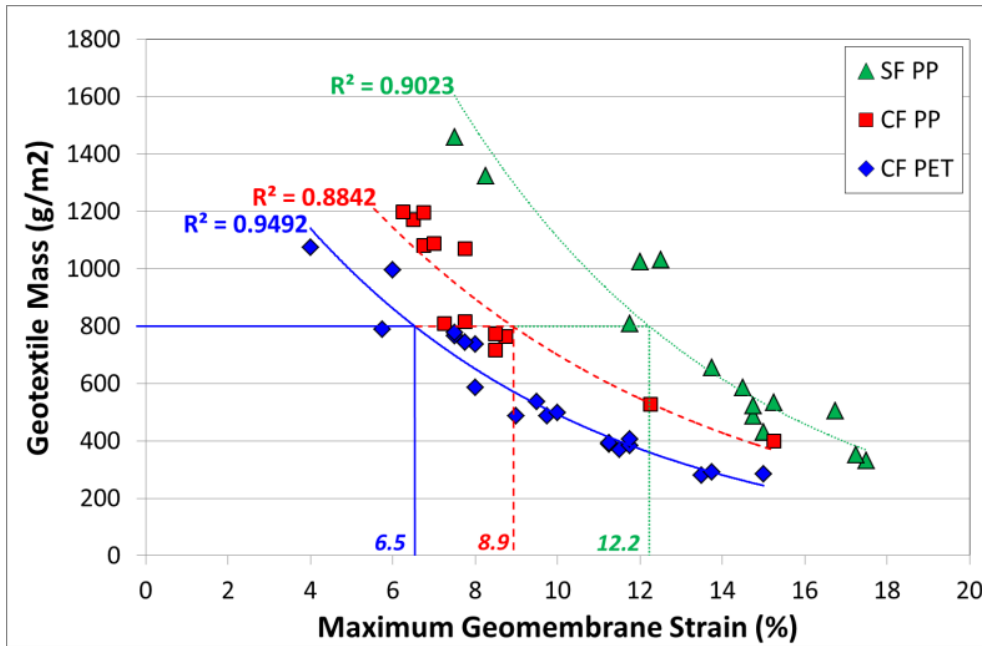


Figure 4. Mass vs. strain relationship for different geotextile groups

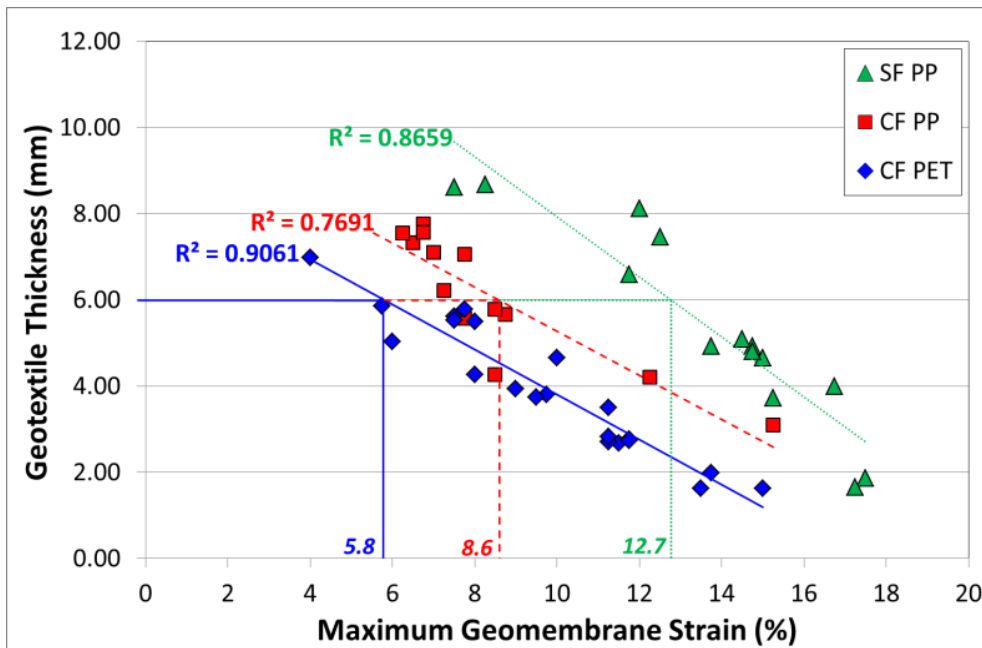


Figure 5. Thickness vs. strain relationship for different geotextile groups

The data clearly show lower overall maximum strain values for the continuous filament geotextiles. It is theorized that local strain may be reduced in these cases due to the continuous nature of the fibres in such products, as opposed to short-cut staple fibres which have an increased proclivity to separate under load (Figure 6). Differences in fibre strand tenacity, elongation, crimp levels and needling may also be factors influencing the cushioning performance of different geotextiles.

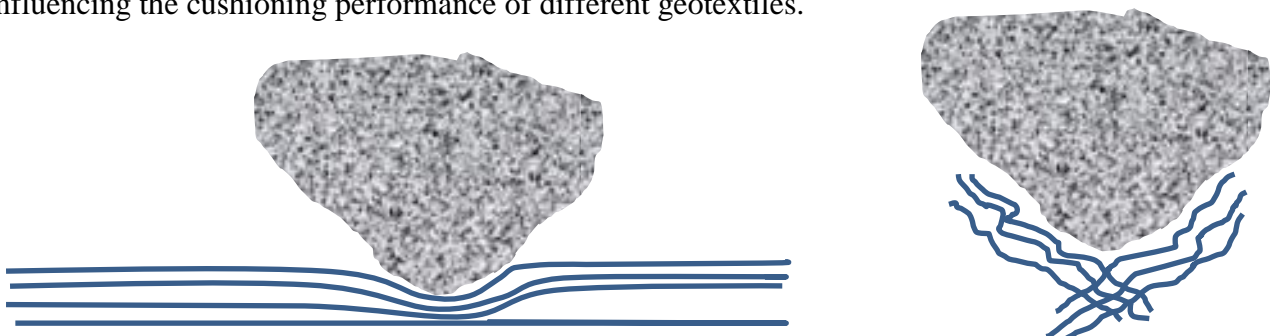


Figure 6. Stone protruding into Continuous Filament vs. Staple Fibre Geotextile

2.2 Influence of Polymer Type

Based on the population of test data, it is evident that different polymer types behave differently to the particular type of point loading associated with this method. It is possible that the density of the polymers play a key role in the reduction of localised strain values. The density of Polypropylene (~0.91g/cc) is much lower than that of Polyester (~1.38 g/cc). By way of analogy, consider the differences between two cylinders; a low density foam cylinder representing an individual Polypropylene fibre and a solid rubber cylinder representing an individual Polyester fibre placed on a firm subgrade. As localised point pressure is applied, the foam cylinder will have a higher compressibility than the rubber under identical loads, yielding a higher overall strain. This increase in strain is then transmitted to the subgrade. It is conceivable that differences in crystallinity and polymer structure may also play a role in geomembrane protection efficiency but further research is required.

3 CONCLUSIONS

The analysis presented above highlights the differences in geomembrane protection efficiency for a variety of different geotextiles. While geotextile mass and thickness have been used historically as indicators for geomembrane protection efficiency, current research suggests that geotextile selection should be assessed beyond these parameters alone. It is evident from the results that continuous filament geotextiles are able to provide a higher resistance to liner strain than staple fibre geotextiles. This may be due, in part, to the continuous nature of the fibres in conjunction with the laydown and needling processes. Staple fibres are short and crimped and have an increased potential for higher localised liner strain, as demonstrated in the test results. Additionally, from the testing undertaken to date, it appears that polyester geotextiles provide additional protection to the geomembrane over polypropylene geotextiles. It is postulated that the higher density of the polyester fibres may contribute to lower overall strains in the geomembrane samples.

REFERENCES

ASTM D5514-06, Standard Test Method for Large Scale Hydrostatic Puncture Testing of Geosynthetics, 2011.

W P Hornsey and D M Wishaw. 'Development of a methodology for the evaluation of geomembrane strain and relative performance of cushion geotextiles'. Geotextiles and Geomembranes 35 (2012) Page 87-99.

W P Hornsey and E M Gallagher. 'Developments in measurement of geomembrane strain and performance of cushion geotextiles for liner protection analysis'. Proceedings EuroGeo 5, 2012.

W.P Hornsey, Performance of cushion geotextiles for liner protection applications. Proc. 2nd African Conference of Geosynthetics, 2013.